REPORT DOCUMENTATION PAGE

Form Approved
OMB No. 0704-0188

PLEASE DO NOT RETURN YOUR FORM TO THE ABOVE ADDRESS.

1. REPORT DATE *(DD-MM-YYYY)*	2. REPORT TYPE	3. DATES COVERED *(From - To)*
09-17-2004	Final	4 April 1997 to 30 September 2003

4. TITLE AND SUBTITLE
RF Photonic Material and Devices

5a. CONTRACT NUMBER

5b. GRANT NUMBER
N00014-97-1-0508

5c. PROGRAM ELEMENT NUMBER

6. AUTHOR(S)
Ming C. Wu (P.I.)
Harold Fetterman, Tatsuo Itoh, Bahram Jalali, Eli Yablonovitch,
Larry R. Dalton, William H. Steier, Connie Chang-Hasnain, Kam Lau,
Rajeev Ram

5d. PROJECT NUMBER

5e. TASK NUMBER

5f. WORK UNIT NUMBER

7. PERFORMING ORGANIZATION NAME(S) AND ADDRESS(ES)
University of California, Los Angeles (UCLA)
Electrical Engineering Department
420 Westwood Plaza
Los Angeles, CA 90095-1594

8. PERFORMING ORGANIZATION REPORT NUMBER

9. SPONSORING/MONITORING AGENCY NAME(S) AND ADDRESS(ES)
U.S. Navy/ Office of Naval Research
Ballston Centre Tower One
800 North Quincy Street
Arlington, VA 22217-5660

10. SPONSOR/MONITOR'S ACRONYM(S)
ONR

11. SPONSOR/MONITOR'S REPORT NUMBER(S)

12. DISTRIBUTION/AVAILABILITY STATEMENT
Distribution: Approved for public release

13. SUPPLEMENTARY NOTES

20041008 493

14. ABSTRACT
Our MURI research team has developed several innovative materials and devices that would enable a quantum leap in the performance of RF Photonic systems. We have also applied these devices to several novel system concepts and achieved world record performances. In the material development, we have produced new electro-optic polymers with record high electro-optic coefficients (r33 = 60 pm/V at 1330 nm and 45 pm/V at 1550 nm wavelengths), low optical loss (< 2 dB/cm), and good long-term stability at 100°C. This leads to electro-optic polymer modulators with record low Vpi (1.2 V @ 1300 nm and 1.8V @ 1550 nm) and high bandwidth (> 40 GHz, limited by the measurement systems). On the receiver side, we have developed a series of innovative high power traveling wave photodetectors, including a distributed balanced photodetector with a record noise suppression (43 dB) over a broad frequency range, a parallel-fed velocity-matched distributed photodetector with a very high linear photocurrent (52 mA), and a novel backward-wave-cancelled traveling wave photodetector with 38 GHz bandwidth and 6-dB enhancement of RF efficiency. We have also demonstrated a new balanced electroabsorption modulator concept that enables us to simultaneously cancel the second- and the third-order distortions. Using these components, we have successfully demonstrated a novel time-stretched photonic analog-to-digital converter. A record high sample rate of 120 Gsamples/second has been achieved.

15. SUBJECT TERMS

16. SECURITY CLASSIFICATION OF:			17. LIMITATION OF ABSTRACT	18. NUMBER OF PAGES	19a. NAME OF RESPONSIBLE PERSON
a. REPORT	b. ABSTRACT	c. THIS PAGE			Dr. Ming C. Wu
U	U	U	UU	42	19b. TELEPHONE NUMBER *(Include area code)* (310) 825-6859

Final Report

RF Photonics Materials and Devices

ONR MURI Award Number: N00014-1-508

Principal Investigator:

Ming C. Wu
University of California, Los Angeles

Co-Principal Investigators:

University of California, Los Angeles:
Harold Fetterman
Tatsuo Itoh
Bahram Jalali
Eli Yablonovitch

University of Southern California:
William H. Steier

University of Washington:
Larry R. Dalton

University of California, Berkeley:
Connie Chang-Hasnain
Kam Lau

Massachusetts Institute of Technology:
Rajeev Ram

1. Table of Contents

2. Abstract:

Our MURI research team has developed several innovative materials and devices that would enable a quantum leap in the performance of RF Photonic systems. We have also applied these devices to several novel system concepts and achieved world record performances. In the material development, we have produced new electro-optic polymers with record high electro-optic coefficients (r33 = 60 pm/V at 1330 nm and 45 pm/V at 1550 nm wavelengths), low optical loss (< 2 dB/cm), and good long-term stability at 100°C. This leads to electro-optic polymer modulators with record low Vpi (1.2 V @ 1300 nm and 1.8V @ 1550 nm) and high bandwidth (> 40 GHz, limited by the measurement systems). On the receiver side, we have developed a series of innovative high power traveling wave photodetectors, including a distributed balanced photodetector with a record noise suppression (43 dB) over a broad frequency range, a parallel-fed velocity-matched distributed photodetector with a very high linear photocurrent (52 mA), and a novel backward-wave-cancelled traveling wave photodetector with 38 GHz bandwidth and 6-dB enhancement of RF efficiency. We have also demonstrated a new balanced electroabsorption modulator concept that enables us to simultaneously cancel the second- and the third-order distortions. Using these components, we have successfully demonstrated a novel time-stretched photonic analog-to-digital converter. A record high sample rate of 120 Gsamples/second has been achieved.

3. Overview:

3.1. Introduction

Photonics is an important enabling technology for the generation, processing, and distribution of microwave signals. Many RF photonic systems have been proposed or demonstrated, however, the RF performances of most systems did not satisfy the requirements due to limit in materials and devices. Under the sponsorship of Office of Naval Research (ONR), we have organized a vertically integrated Multidisciplinary University Research Initiative (MURI) team from four universities (UCLA, USC, UC Berkeley, and MIT) to address the critical material and device issues in RF photonics. In this paper, we report on our recent achievements in electro-optic polymer materials; wideband, low-voltage polymer modulators; distributed balanced photodetectors; balanced electroabsorption modulators; analog vertical cavity surface-emitting lasers; planar integrated antennas for photonic-microwave conversions; and arbitrary waveform generations.

3.2. Polymer Electro-optic Modulators

Our research has focused on exploiting the concepts of nanoscale architectural engineering to design and synthesize new materials characterized by record electro-optic activity. Nanoscale supremolecules called dendrimers because of their branched "tree-like" appearance have been prepared that yield record electro-optic activities of 60-90 pm/V at 1.55 μm. Proton concentration is readily controlled in these materials (in

contrast to polymer materials) leading to low proton density materials and low optical loss (0.2 dB/cm) at telecommunication wavelengths (1.55 μm). Nano-engineered dendrimers also exhibit better processability including solubility in spin casting solvents. They are easily interclated into photonic bandgap lattices to prepare voltage-controlled wavelength selective filters for applications such as WDM. They are readily crosslinked to yield hardened lattice for the improvement in thermal and photostability. In the past, organic electro-optic materials consisted of chromophores and "everything else" with no thought given to the "'everything else". Dendrimers provide a route to making the "everything else" contribute to desired properties ranging from electro-optic activity, to optical loss, to stability.

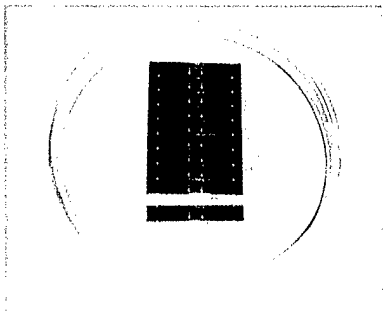

Figure 3.2-1: Photograph of 10 Mach-Zehnder modulator on 3-inch wafer with Vπ(dc) of 1.2 V @ 1300 nm, 1.8 V @1550 nm and 3-dB bandwidth of 15 GHz and 35 GHz, respectively.

Using the new polymer materials, dramatic advances in practical high-speed polymer electro-optic modulators have been achieved. Traveling wave push-pull modulators (Figure 3.2-1) with Vπ of 1.2 V @ 1300 nm and 1.8V @ 1550 nm have been demonstrated. These devices have a 2 cm long interaction length and have a measured 3-dBe bandwidth of 15 GHz. Similar devices with shorter interaction length and higher Vπ have a bandwidth of 35 GHz. The success of these modulators is based on a new understanding of the chemistry of electro-optic polymers, new fabrication procedures, and the integration of guided wave optics and guided wave electronics. Great progress has also been made in issues relating to the long-term stability of polymer photonic devices. We have demonstrated long-term photo-stability by excluding free oxygen in the packaging and made progress on improved long-term thermal stability. An effort is now underway to bring these devices to market.

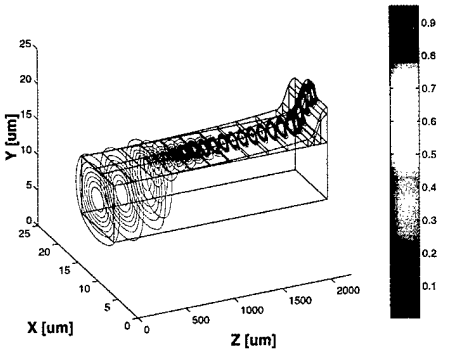

Figure 3.2-2: scale drawing of the transition structure with optical intensity contours from a 3-D vectoral simulation superimposed.

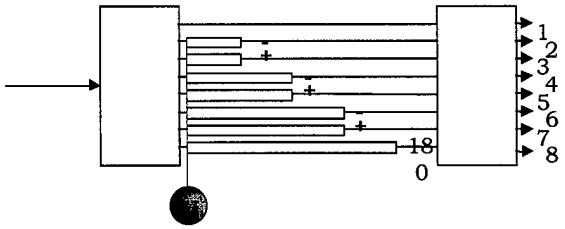

Figure 3.2-3: schematic of a 1x8 switch, taking advantage of MMI phase relation symmetries and the ability to oppositely-pole electro-optic polymers for single drive voltage switching.

During the last year we have made new high frequency optoelectronic oscillators working at 40 GHz. These devices have extremely low phase noise and use our new polymer materials in a push - pull configuration. The devices have been configured to use Mach Zehnder structures which have low $V\pi$ and freedom from chirp. We have now started to look at the use of our latest CX-2 materials in conjunction with passive guides. We are using SiO_2 as the passive material and novel vertical transition, using gray scale masks, to our active materials. This design should yield entirely new devices which will completely eliminated many of the problems with optical losses that have been associated with polymer systems. In Figure 3.2-2 we show the basic vertical transition and in Figure 3.2-3 we show a push-pull 1XN switch that will work at 40 GHz using this approach.

3.3. Distributed Balanced Detectors

The RF performance in externally modulated fiber optic links, including noise figure (NF) and spurious-free dynamic range (SFDR), improves with increasing optical power until the noise is limited by laser relative intensity noise (RIN). Balanced RF photonic links suppress RIN through balanced detection and offer superior RF performance. Balanced photodetectors with high linearity and high saturation power are the key enabling components. Most monolithic balanced photodetectors reported in the literature are optimized for digital systems and have relatively low saturation power (~ 1 mW).

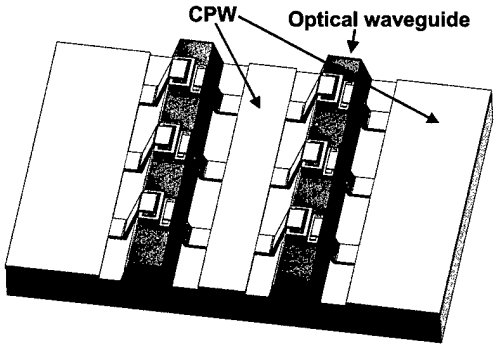

Figure 3.3-1: Schematic of distributed balanced photodetector with p-i-n photodiodes.

Previously, we have proposed a novel distributed balanced photodetector that integrates velocity-matched distributed photodetector (VMDP) with balanced detectors. This concept has been demonstrated using metal-semiconductor-metal (MSM) photodiodes. However, MSM photodiodes suffer from catastrophic damage at low power. P-i-n photodiodes have higher power handling capability due to larger potential barrier for dark current and more uniform electric field distribution. Recently, we have successfully developed a new technology to integrate p-i-n photodiodes and passive optical waveguides with low transition loss. We have achieved a record-high linear photocurrent of 45mA using this structure. No thermal runaway was observed for photocurrent above 55 mA. We have successfully fabricated a distributed balanced photodetector with p-i-n photodiodes with flat frequency response from 1 to 35 GHz. Using this receiver in a balanced link, we demonstrate that the intensity noise, including RIN and erbium-doped fiber amplifier-added noise, has been suppressed by as much as 43 dB over a broad frequency range (1 to 12 GHz) [3].

3.4. Balanced Electroabsorption Modulators

Conventional balanced links employ cross-coupled Mach-Zehnder modulators (X-MZM). Such links suffer from high SFDM because the X-MZM needs to be biased at the maximum of third-order distortion. We have proposed a novel balanced electroabsorption modulator (B-EAM) to overcome this problem. The schematic of B-EAM is shown in Figure 3.4-1. It consists of a pair of serially connected electroabsorption modulators, and the RF signal is applied to the center electrode.

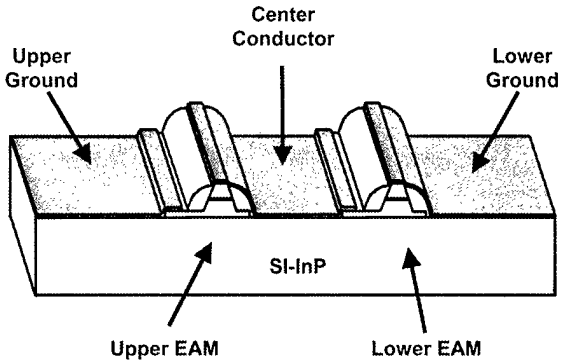

Figure 3.4-1: Schematic of balanced electroabsorption modulator (B-EAM).

A novel balanced electroabsorption modulated photonic link for simultaneous suppression of even order distortions, 3rd order distortions, laser RIN, and common amplified spontaneous emission noise at the same modulator bias point was experimentally demonstrated for the first time. By biasing at the third order null, the 3rd order distortions can be suppressed, while the balanced link architecture suppresses all even-order distortions and common mode noises. The fabricated balanced electroabsorption modulator (B-EAM) showed well-matched DC characteristics in terms of I-V and transfer curve. System experiments were performed to compare Single-EAM and B-EAM links. By biasing the B-EAM at the 3rd order null and operating the link in balanced mode, 7.5 dB suppression of 2nd order distortion and 2 dB suppression of laser RIN at the RIN peak (910 MHz) was experimentally demonstrated. The two-tone measurement showed 17 dB suppression of 2nd order distortion and 20 dB improvement in SFDR compared to the Single-EAM link [3].

3.5. Planar Antennas for Photonic-Microwave Conversion

Antennas printed on high dielectric constant substrates typically suffer from undesired effects due to generation of surface-waves, including low radiation efficiency, high cross-pol radiation, and strong mutual coupling. In complete contrast, the proposed novel printed quasi-Yagi antenna [5] takes advantage of the generation of surface-waves. This fact makes it ideal for construction on III-V materials such as GaAs and InP. The same antenna structure has been successfully demonstrated as a low loss microstrip-to-waveguide transition [6]. Integration of the quasi-Yagi antenna and VMDP offer the flexibility of being able to collect generated microwave power into metallic waveguides or launch it directly into free-space for applications such as quasi-optical power combining. We can use the odd-symmetric nature of the VMDP to generate the balanced field configuration needed to excite the driver dipole directly. This structure is also able to provide heat sinking through the metal backing under the coupled lines while still ensuring broadband operation and unidirectional radiation. The X-band prototype of the back-to-back coupled line-to-waveguide transition exhibits a bandwidth of 26% for return loss less than –10dB (Figure 3.5-1). The insertion loss ranges from –0.5 to –1.2 dB.

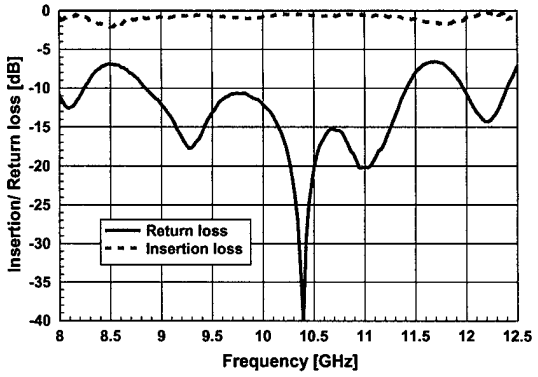

Figure 3.5-1: Measured results of back-to-back coupled microstrip line to waveguide transition.

3.6. VCSEL performance in RF photonic links

Our measurements of short free space RF links using multimode vertical cavity surface-emitting lasers (VCSELs) demonstrated high dynamic range of approximately 100 dB (1Hz bandwidth) at frequencies in the 1-3 GHz range with a maximum measured dynamic range of 110 dB (1Hz bandwidth) at approximately 1GHz. These measurements stimulated some theoretical questions such as what determines the structure of the dynamic range and why do multimode VCSELs have performance comparable to edge emitting lasers. The results of our modeling effort are summarized below.

In a multimode laser, near resonance, modes respond collectively like a single mode laser. At modulation frequencies far below resonance, where the distortion and noise of a single mode laser are low, intermode dynamics play an important role. Mode partitioning increases intensity noise when there is mode selective loss. Distortion is increased when weak modes couple to the dominant lasing modes. Mode selective loss has an effect on low frequency distortion.

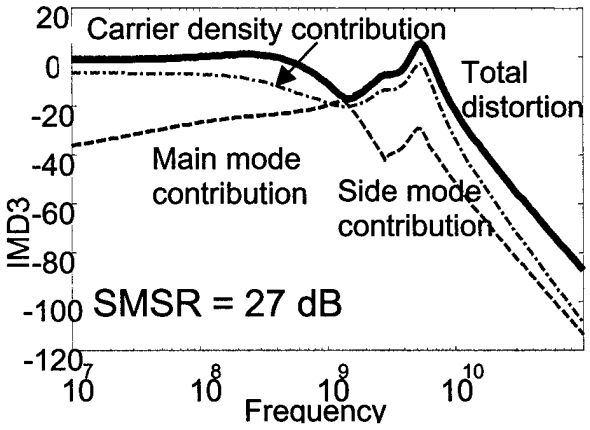

Figure 3.6-1: Third order intermodulation distortion for a two-mode laser with side-mode-suppression-ratio of 27 dB.

Figure 3.6-1 shows the third order intermodulation distortion for a two-mode laser with low mode overlap shown in the upper right quadrant. The contributions to the total intermodulation distortion by the main mode, side mode, and carrier density are shown for three different side mode suppression ratios. For the 36dB SMSR case, the distortion response of an essentially single mode laser because the side mode is too weak to perturb the main mode. For the 27dB case, nonlinear response of the side mode drives the main mode, leading to increased low frequency distortion. When both modes are lasing, the distortion again approaches the single mode case due to improved carrier density clamping from the stimulated emission of both modes.

3.7. References

[1] H. Ma, B. Chen, S. Takafumi, L. R. Dalton, and A. K. Y. Jen, "Highly Efficient and Thermally Stable Nonlinear Optical Dendrimer for Electro-Optics," J. Am. Chem. Soc, 123 (5), 986-7 (2001).

[2] M-C. Oh, H. Zhang, A. Szep, W.H. Steier, C. Zhang, L.R. Dalton, H. Erlig, Y. Chang. Boris Szep, H.R. Fetterman, "Recent advances in electro-optic polymer modulators incorporating phenyltetraene bridged chromophore " (Invited) J. Quant Electr. Sel. Topics on Organics for Photonics, December 2001.

[3] M.S. Islam, S. Murthy, T. Itoh, M.C. Wu, D. Novak, R.B. Waterhouse, D.L. Sivco, A.Y. Cho, "Velocity-matched distributed photodetectors and balanced photodetectors with p-i-n photodiodes," IEEE MTT Special Issue on Microwave and Millimeter Wave Photonics, Vol. 49, pp. 1914 –1920, Oct 2001.

[4] Mathai, et al, "Experimental demonstration of a balanced electroabsorption modulated microwave photonic link," IEEE MTT Special Issue on Microwave and Millimeter Wave Photonics, vol. 49, pp. 1956-1961, Oct. 2001.

[5] W. R. Deal, N. Kaneda, J. Sor,Y. Qian and T. Itoh, "A New Quasi-Yagi Antenna for Planar Active Antenna Arrays,"IEEE Transactions on Microwave Theory Tech., vol. 48, No. 6, pp. 910-918, June, 2000.

[6] N. Kaneda, Y. Qian and T. Itoh, "A Broadband Microstrip-to-Waveguide Transition Using Quasi-Yagi Antenna," IEEE Trans. Microwave Theory Tech, vol. 47, pp. 2562-2567, December 1999.

[7] B. Jalali and I. Newberg, "Photonic Arbitrary Waveform Generator," GOMAC 2002, Paper 12.8.

4. Detailed Scientific Progress and Accomplishments

4.1. High Power Photodetectors for RF Photonics

Scientific Personnel

Prof. Ming C. Wu, Principal Investigator
Prof. Tatsuo Itoh, Co-P.I.
M. Saif Islam, Research Assistant
Tai Chau, Research Assistant

Tom Jung, Research Assistant
Sagi Mathai, Research Assistant

Balanced Distributed Photodetectors:

Balanced receivers are very attractive for high performance microwave photonic links. They can suppress the laser relative intensity noise (RIN) and the amplified spontaneous emission noise (ASE) from erbium doped fiber amplifiers (EDFA). This enables the link to achieve shot noise-limited performance at high optical powers. The link gain, spurious-free dynamic range (SFDR), and the noise figure are greatly improved. To realize these advantages, balanced photodetectors with high saturation photocurrents and broad bandwidth are needed.

Though discrete balanced photodetectors with high saturation power have been reported, their bandwidth is limited. Monolithically integrated balanced photodetectors offer superior performance (broader bandwidth, better matching of photodiodes) and reduced packaging cost. However, most of the reported integrated balanced receivers suffer from low saturation power and are not suitable for analog links. We report here on a improved monolithic distributed balanced photodetector that has a maximum linear DC photocurrent of 33 mA (equivalent to 66 mA from regular, non-balanced photodetectors). We achieved high AC linearity of devices under high power operations.

Figure 4.1-1(a) shows scanning electron micrograph (SEM) of the distributed balanced photodetector. It consists of two input optical waveguides, two arrays of high-speed metal-semiconductor-metal (MSM) photodiodes distributed along two passive optical waveguides, and a 50Ω coplanar waveguide (CPW) microwave transmission line. The detector operates in balanced mode when a voltage bias is applied between the two ground electrodes of the CPW. The photodiode arrays provide periodic capacitance loading to slow down the microwave velocity. The photodiodes are designed to operate below saturation under high optical input by coupling only a small fraction of light from the passive waveguide to each individual photodiode.

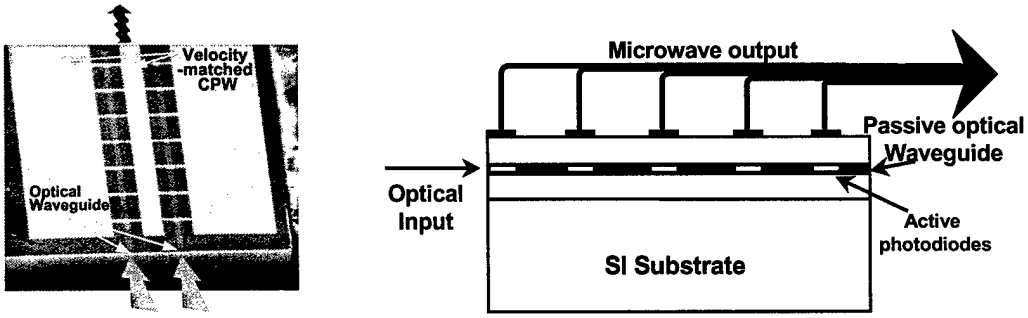

Figure 4.1-1 (Left) SEM micrograph of the distributed balanced receiver. MSM photodiodes are distributed along the optical waveguide. (Right) Principal of power combining on each branch of the receiver.

The primary improvements we have made this year in this device are (1) continuous waveguide transitions between passive guide and active photodiodes, and (2) multimode optical waveguides. In our previous devices, the optical waves were weakly confined by ridge structures, and the discontinuity of the waveguide width also resulted in excessive optical loss at the waveguide transitions. Here, we employed a strong index-guided optical waveguide with uniform width for both the active photodiode and the passive waveguide. Particular care has been taken to ensure the continuity of the MSM fingers across the 1.5-μm-high waveguide.

We have also employed a 5-μm-wide multimode waveguide to increase the saturation optical power. Multimode waveguide has been employed in lumped waveguide photodetectors to improve fiber coupling efficiency. Here, we observed almost three-fold improvement in the maximum photocurrent level of the multimode waveguide distributed photodetectors with respect to single mode waveguide devices in our first demonstration. This is an indication of better guiding and uniform distribution of input power to multiple photodiodes in the receiver.

The balanced receiver exhibits very good electrical and optical characteristics. The dark current is measured to be <0.2 nA/diode at 10 V bias. The DC response is found to be flat above 4V bias. The responsivity is 0.28A/W at 4V bias (without AR coating). Figure 4.1-2 shows measured photocurrent in one branch of the photodetector versus the input optical power. The photocurrent remains linear up to 33mA. The device fails at higher photocurrent due to thermal runaway. It should be noted that the 33mA photocurrent in balanced photodetector is equivalent to 66mA photocurrent in single-ended photodetectors because the RF signals from both branches of photodiodes add in phase.

In order to investigate the AC nonlinearity of the distributed photodetectors, we used two-tone modulation method. Optical heterodyning of three external-cavity tunable lasers were employed to generate two RF tones at 13 and 14.5 GHz on one branch of the balanced receiver. The output of the receiver was directly connected to a microwave spectrum analyzer. We did not observe any 2nd or 3rd order harmonics (H2 or H3) or 3rd order intermodulation distortion with photocurrent as high as 20 mA (limited by our setup). This demonstrates the high AC linearity of the receiver.

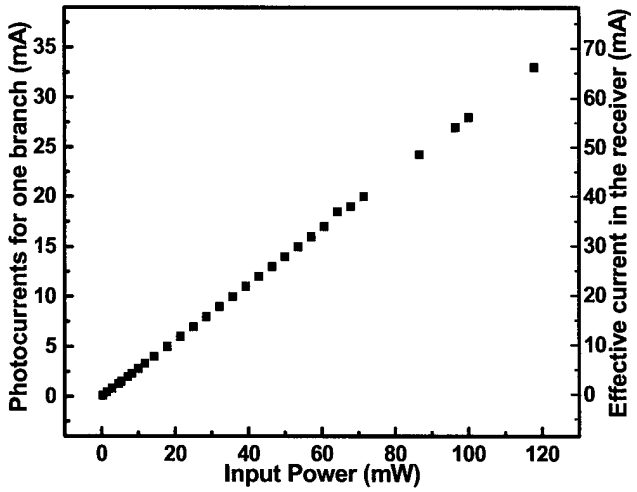

Figure 4.1-2 DC photocurrent versus input optical power. The DC photocurrent remains linear up to 33mA.

The frequency response of a single branch of the photodetector was measured under various optical input powers. The bandwidth of the photodetector remained unchanged (14.5 GHz) when the photocurrent is varied from 0.5 mA to 14.5 mA. Figure 4.1-3(a) shows the AC response of the phodetector at RF frequencies of 10 and 15 GHz versus the photocurrent. The AC response is proportional to the square of the photocurrent up to the highest photocurrent measured (14.5 mA, limited by the setup). This confirmed the linearity of the photodetector.

To investigate the AC linearity of the receiver in balanced mode, we designed a setup as described below. An external cavity tunable laser with 1550-nm wavelength and 3 dBm output power is employed as the optical source. It is amplified by an EDFA and then filtered by an optical bandpass filter with 2-nm bandwidth. The microwave signal was modulated onto the optical carrier by an X-coupled Mach-Zehnder modulator (MZM), which produces two complimentary outputs. The outputs are coupled to the balanced receiver by two lensed fibers. Another external cavity laser is employed to provide additional DC input. It is similarly amplified by another EDFA, split into two equal branches and then combined with the AC signals through two 3dB couplers. The wavelengths of the external cavity lasers are separated far enough to avoid interference of their beating frequency. The polarization orientations of both AC and both DC signals are independently optimized by four polarization controllers. The AC photocurrents were set to 160 μA for each branch of the receiver and the DC currents were allowed to vary from 1 mA to 13 mA (limited by our setup). Figure 4.1-3(b) shows the AC output power versus the DC photocurrent at a frequency of 13.5 GHz. In this photocurrent range, the AC signal remained equal in magnitude within an experimental error of half a dB. To our knowledge, this is the first report of the AC linearity measurement of balanced receivers.

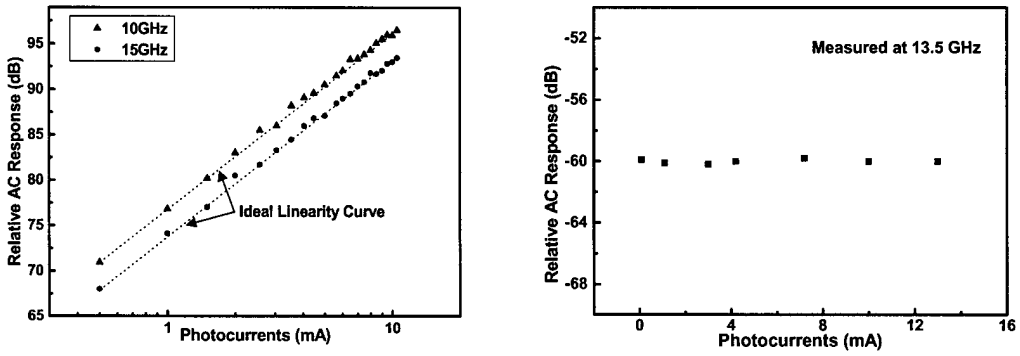

(a) (b)

Figure 4.1-3 (a) Meaured AC linearity of the balanced receiver at different photocurrents. The dotted line shows the ideal linearity curves. (b) Measured AC response of the balanced receiver at different photocurrent level. The response is linear at the photocurrent range within the experimental error of 0.5 dB.

For optimum RF link performance, high power receivers must maintain their high-speed performance at high DC photocurrents. Most photodiodes suffer from degradation in the frequency response at high photocurrents due to the electric field screening effect. Using the setup described before, we measured the AC response of the balanced receiver at various photocurrent levels. No DC input was used in this measurement. Figure 4 shows the relative AC responsivity of the balanced receiver with photocurrents varying from 0.5 mA to 10.5 mA. The frequency response at 10.5 mA is identical to that at 0.5 mA, indicating excellent linearity of the balanced receiver at high photocurrent. The 3-dB bandwidth of the balanced receiver (13.8 GHz) is slightly lower than that of the individual branches (14.5 GHz). This may be due to parasitics of the biasing capacitor (120 pF) on one ground of the probe for DC biasing and RF signal collection.

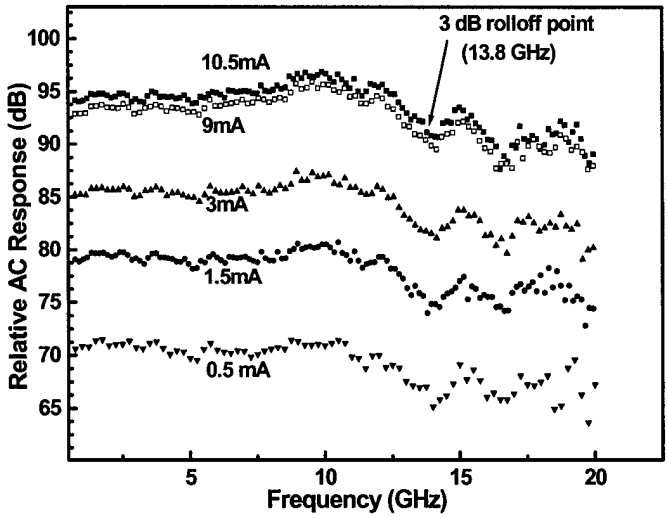

Figure 4.1-4 Measured frequency response of the distributed balanced receiver at various DC photocurrents.

In conclusion, we have successfully demonstrated a distributed balanced photodetector with high photocurrent and excellent linearity. It has a maximum linear DC photocurrent of 33 mA (equivalent to 66 mA in single-ended photodetectors). The device also exhibited excellent AC linearity at high photocurrents. The experimental results indicate that the distributed balanced photodetector will have a major impact on high performance RF photonic systems.

Parallel-Fed Distributed Photodetectors

Most of the distributed diodes are in series (SF-VMDP) and fed by a single optical waveguide. Due to the exponential nature of photoabsorption, the first photodiode in the chain generates the highest photocurrent and fails while the remaining discrete diodes are still operating at current levels below their failure thresholds. As a result, the maximum linear photocurrent of the SF-VMDP is limited by thermal runaway induced failure of the first photodiode. The increase in absorption volume due to velocity matching is, thus, not fully utilized.

We have proposed and demonstrated a parallel feed velocity-matched distributed photodetector (PF-VMDP) to achieve equal photocurrents in the N distributed diodes, as shown in Figure 4.1-5(a). The photocurrents in all the diodes are equal and in case of failure, all the diodes in the detector reach their failure threshold current limit simultaneously. By separating the individual photodiodes by more than the thermal crosstalk distance, the maximum photocurrent for thermal runaway is greatly increased. In addition, we also reduce the peak photocurrent density by the splitting ratio, N, which decreases saturation effects caused by charge screening. The electrical outputs of these N photodiodes are still collected in phase through a velocity matched coplanar microwave transmission line to maintain high bandwidth. PF-VMDP thus enables us to fully utilize the absorption volume to achieve higher linear photocurrents without sacrificing bandwidth.

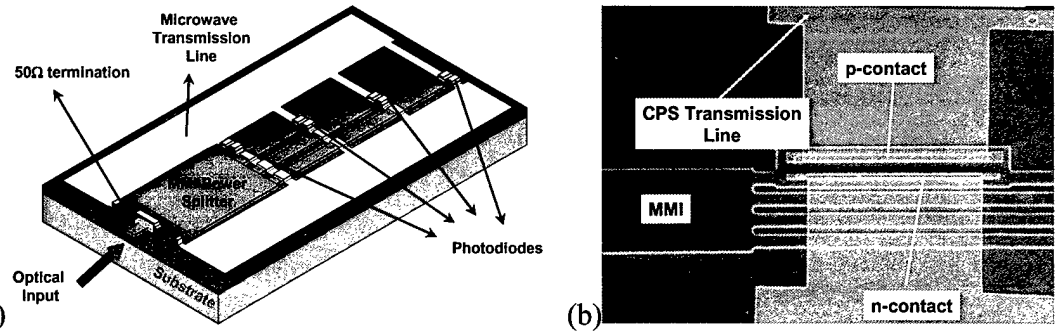

Figure 4.1-5 (a) Schematic and (b) SEM of parallel-fed velocity-matched distributed photodetectors (PF-VMDP).

The dark current of the p-i-n PF-VMDP is less than 1μA at –2V bias. The responsivity of the PF-VMDP detector shows is 0.21A/W. The DC photocurrent is linear up to 52.2mA (Figure 4.1-6). To our knowledge, this is the highest reported DC photocurrent for

1.55μm detectors. This current is limited by the maximum possible output of our erbium-doped fiber amplifier (EDFA). We believe we can reach even higher linear photocurrents, either by increasing the optical input to the detector or by improving the responsivity of our detector with an integrated spot-size converter.

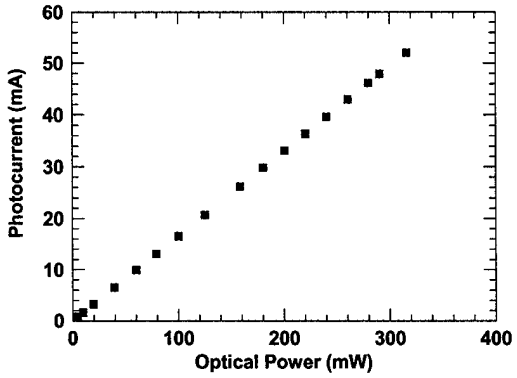

Figure 4.1-6. DC response of the parallel-fed velocity-matched distributed photodetector (PF-VMDP). The maximum linear photocurrent is 52.2 mA.

A high-power optical heterodyne source is used to measure the RF linearity of the PF-VMDP. Two Photonetics external-cavity diode tunable diode lasers whose optical wavelengths are set to be 10GHz apart produce the optical signals for PF-VMDP, and the output is monitored by an HP8565E RF spectrum analyzer. The result is shown in Figure 4.1-7. The maximum linear RF power of 9dBm is also limited by the available optical power in our setup.

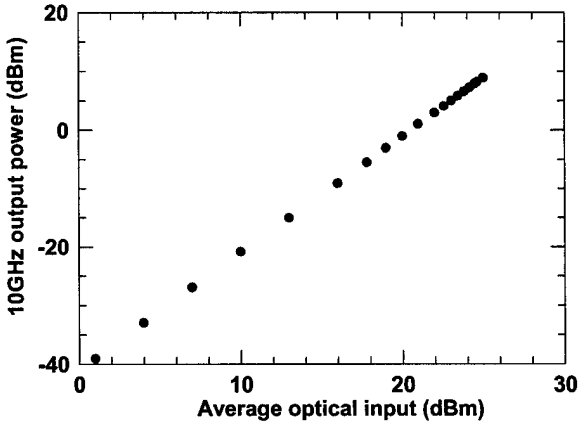

Figure 4.1-7 Optically heterodyned RF output power at 10 GHz versus the average optical input power. The response is linear up to 9 dBm of RF power, limited by the available optical power.

Backward-Wave-Cancelled Traveling Wave Photodetectors

One of the fundamental issues for traveling wave photodetectors is the backward propagating waves generated by the photocurrent. The input ends need to be terminated with the line impedance (usually 50Ω), otherwise the phase lag between the forward and the reflected backward propagating waves will limit the bandwidth. Bandwidth improvement with input termination is, however, at the expense of efficiency as half of the currents generated by the individual photodiodes are dissipated in the 50Ω input termination.

High bandwidth without loss of responsivity can be obtained by canceling the backward propagating wave using the reflections in a multi-section transmission line, as originally proposed for distributed amplification in traveling wave tubes. The schematic of the proposed traveling wave photodetector with backward wave cancellation is shown in Figure 4.1-8. It consists of an array of photodiodes connected by a passive optical waveguide. The photocurrents are collected in a multi-section microwave transmission line. The impedance mismatch at the junction of the different CPS sections creates a partial reflection of the forward propagating wave. The reflection coefficient at each discontinuity is always negative provided the impedances of the multi-section transmission line are tapered down towards the output end (i.e., the load). It is thus possible to use the reflected wave to cancel out the backward propagating fraction of the photocurrent generated by the photodiode at the discontinuity.

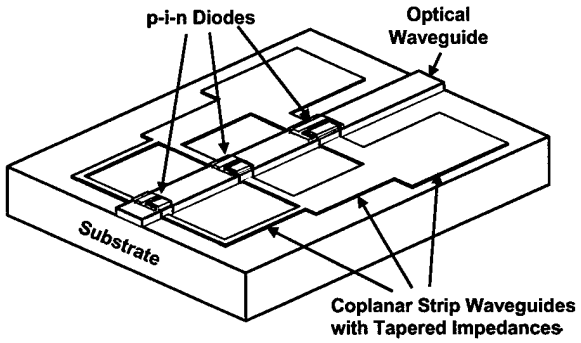

Figure 4.1-8 Schematic of the backward-wave-cancelled traveling wave photodetectors. The backward propagating waves are cancelled exactly by the reflections at the discontinuity of the transmission lines at the photodiodes. The RF efficiency is improved by 6 dB.

We choose to use three discrete diodes with equal photocurrent distribution. The required line impedances of the individual sections of the multi-section transmission line are thus 150Ω, 75Ω and 50Ω from input to output. The widths of the coplanar lines are 2 μm, 40 μm, and 120 μm and the separations between signal and ground electrodes are 120μm, 100μm, and 60μm, respectively. The spacing between the diodes is chosen to be 300μm such that the impedances of the loaded transmission lines are 150Ω, 75Ω and 50Ω. The SEM of the fabricated device is shown in Figure 4.1-9.

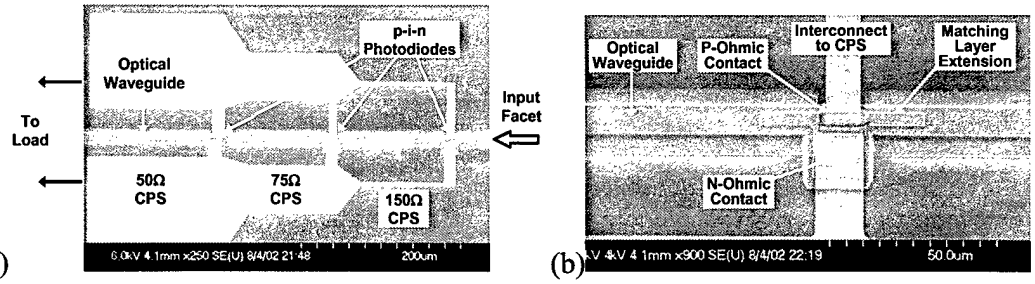

Figure 4.1-9 (a) SEM of the backward-wave cancelled traveling wave photodetector. (b) SEM of the p-i-n photodiode.

The frequency response measured at 0dBm input optical power and –2V bias is shown in Figure 4.1-10. The 3dB bandwidth is 38GHz. The measured bandwidth is 2.5 times higher than the round trip time bandwidth limit of 15 GHz. This confirms that the backward wave in our MS-TWPD is indeed cancelled. Backward wave cancellation enables us to achieve high bandwidth in traveling wave distributed photodetectors without losing 6 dB of electrical power in the input termination resistor. With backward wave cancellation, the necessity of fabricating an on-chip termination resistor and DC blocking capacitor no longer exist, simplifying the fabrication process.

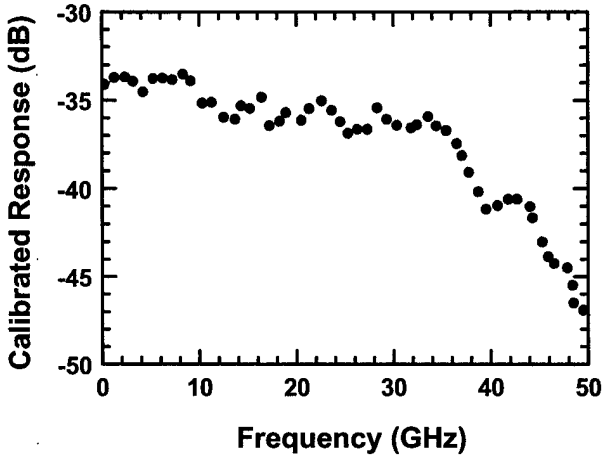

Figure 4.1-10. Frequency response of the backward-wave-cancelled traveling-wave photodetector. A bandwidth of 38 GHz has been achieved, and the RF response is improved by 6 dB.

4.2. Electro-Optic Polymer Modulators

Scientific Personnel
Prof. Larry Dalton, Co-P.I.
Prof. William H. Steier, Co-P.I.
Dr. M-C Oh, Research Associate
H. Zhang, Research Assistant
C. Zhang, Research Assistant

G. Todorova, Research Assistant

Advances in EO Polymers

Professor Larry Dalton has continued the development of polymers with large electro-optic coefficients and Professor Steier in collaboration with Professor Harold Fetterman at UCLA has used these materials in high speed infrared modulators. Dalton's group has recently developed a new chromophore, CLD, with aminophenyltetraene as donor-bridge and a tricyano derivatized furan as acceptor which shows exceptionally high nonlinearity. This chromphore has also been sterically designed with additional side group to prevent the close approach of the molecules and therefore to prevent the dipole-dipole interactions from locking the molecules into a counter alignment. These advances have brought the r33 coefficients in both guest-host and covalently attached crosslinked systems to new levels.

Lockheed has recently identified a very promising polymer host material, APC(amorphous polycarbonate), which has low loss both at 1300 nm and 1550 nm and easily produces high quality, stable thin films. Using this material and the CLD chromophore in a guest host system, we have produced the best polymer modulators yet reported at 1300 and 1550 nm. We have measured the r33 coefficient at 1060 nm as a function of the chromophore loading density. The peak value is approximately 90 pm/V which, when dispersion is taken into account, becomes ~ 60 pm/V @ 1300 nm and ~45 pm/V @ 1550 nm. The optical loss has been measured in a slab waveguide as ~ 1.5 dB/cm @ 1300 nm and ~2 dB/cm @ 1550 nm. The thermal stability break point in poled material was 120°C indicating that long term stability can be expected at 90-100°C.

Dendritic Electro-optic Materials: The next Generation of Electro-optic Materials

Professor Larry Dalton, as part of this program, has developed a number of novel dendritic electro-optic materials. These include versions containing multiple chromophores as shown in Figure 4.2-1.

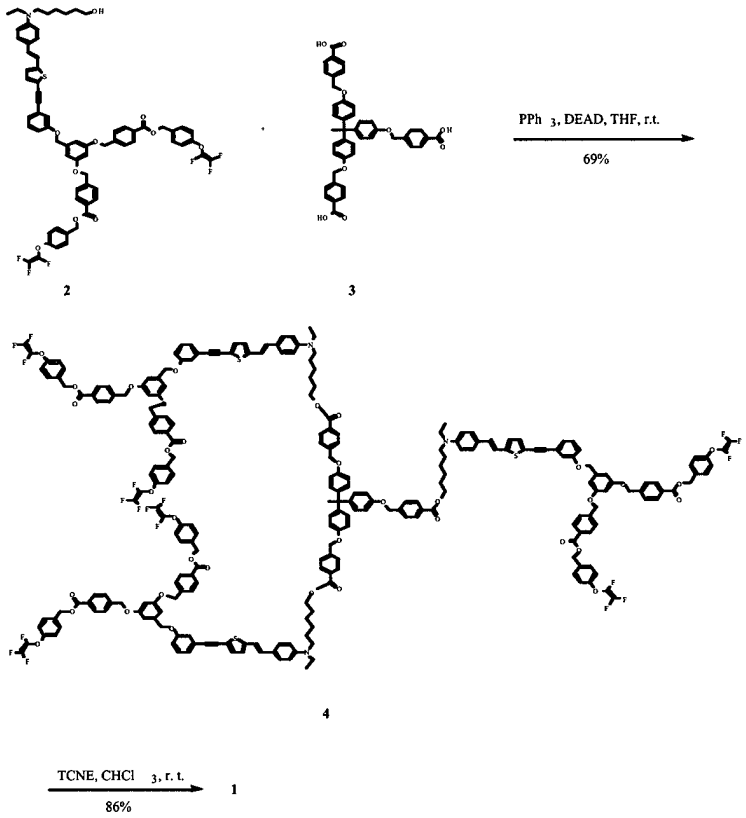

Scheme 2

Figure 4.2-1. A multiple chromophore cross-linkable dentritic EO material

Statistical mechanical (kinetic Monte Carlo) calculations suggest that dendritic structures should permit improved control of inter-molecular electro-static interaction and should result in a significant improvement in electro-optic activity. These structures should also permit improved processing leading to materials with improved thermal and photo-chemical stability. Dendritic materials can also reduce the optical loss by eliminating the absorption due to C-H vibrations.

In a typical example, by fluorination and by use of cyanurate dendron ligands the optical loss has been reduced to 0.4 dB/cm at 1300 nm and 0.1 dB/cm at 1550nm. With modest chromphores (mb <10 x 10-45 esu) an electro-optic coefficient of r33 = 60 pm/V has been achieved. In addition the improved processability has produced crosslinkable versions of demdrimers with r33 stable at 85°C for 1000 hrs. Figure 1 shows an example of multiple chromophore dentritic material.

Advances in Polymer High Speed Modulators

Using the new PC-CLD material we have fabricated some of the best polymer modulators yet reported. We consistently achieved Vpi = 2.5 V @ 1300 nm and Vpi = 3.8 V @ 1550 nm. The interaction length of these devices is 22 mm. In these modulators

we did not achieve as efficient poling as achieved in the test samples. The conductivity of the lower cladding is an issue. With better lower cladding material we expect to further reduce these Vpi number by 70%. Figure 4.2-2 shows the design of the modulator.

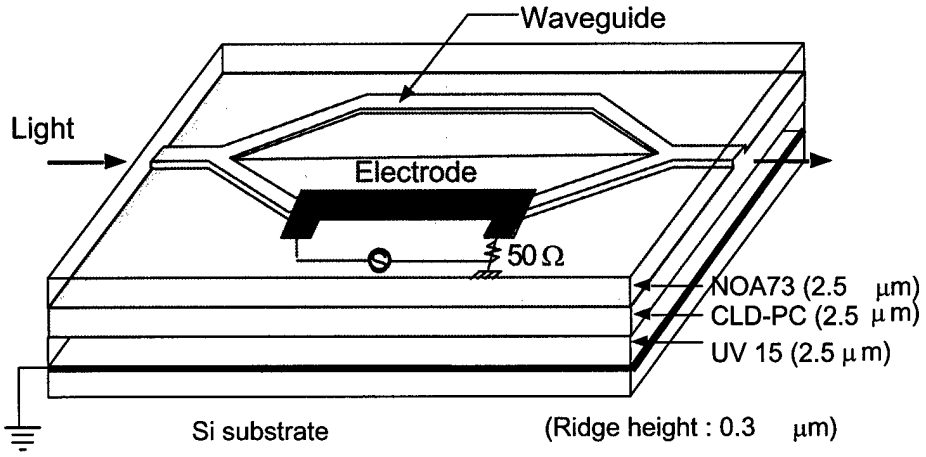

Figure 4.2-2 Polymer microwave infrared modulator.

The measured optical insertion loss of the modulators is 9-10 dB. In this measurement light is butt coupled into the waveguide from a fiber and the output light is collected by a lens and focused onto the detector. We estimate ~ 4 dB input coupling loss and ~1dB of output coupling loss. This leaves 4-5 dB of loss in the modulator which translates into ~1.5 dB/cm loss in the optical waveguides. Our experiments using fiber lenses have shown that the coupling losses can be reduced to ~ 1 dB at the input and the output which will yield a packaged modulator with 6 – 7 dB insertion loss.

The extinct ratio of the modulators is consistently in the 25-30 dB range. This indicates that the waveguides are single mode. Figure 4.2-3 shows the measurement of Vpi.

We have made preliminary frequency response measurement out to 40 GHz and find the response is flat except for ripples due to impedance mismatches in the rf circuit. In a recent time stretching experiment @ 1550nm, Prof. Fetterman's group at UCLA has used these modulators to demonstrate time stretching by a factor of ten from a 100 GHz input down to 10 GHz.

Dr. Y. Shi has recently used the CLD chromophore in a PMMA host to demonstrate a sub 1 V modulator. Using a push-pull poling scheme he measured V = 0.8 V using a 3 cm interaction length.

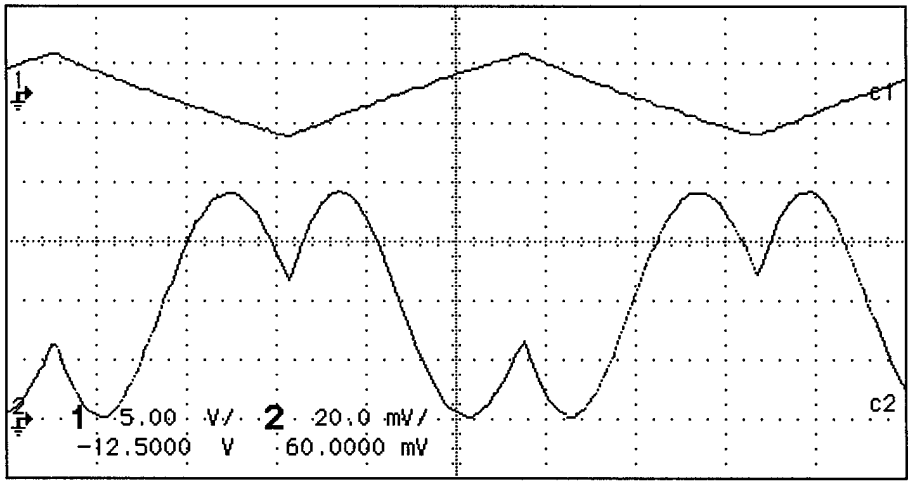

Figure 4.2-3 Measurement of Vpi of the polymer electro-optic modulator. The upper trace is the applied voltage and the lower cure is the 1300 nm light from the modulator

Integrated Polymer Opto-Electronics

We have developed techniques to include our modulators in more complex optical circuits including arrays of modulators and arrays of photonic rf phase shifters. This work is in close collaboration with Professor Fetterman's group at UCLA. One of the major issues is the optical loss in the active polymer material that becomes a serious problem when the length of the waveguides is more then 3-5 cm. One solution is devices that integrate both passive and active polymer materials within the same optical integrated circuit. The goal is to achieve lower over all insertion loss by using the higher loss active polymers only where needed. The general approach is to use adiabatic tapers between the two materials to assure a low loss transition by matching the mode profiles. This builds on earlier work on 3D integrated optics. One of the most promising low loss materials system is the SiO2. The poling and operation of polymer EO device integrated with SiO2 may require going to in-plane poling and a co-planar electrode configuration. .

Industrial Collaboration and Technology Transfer

The MURI team has collaborated with the following companies on research and technology transfer:

1. TACAN, Inc.
2. RVM Scientific
3. Pacific Waves, Inc.

We have met with the following companies to explore possible joint research programs in areas of RF photonics:

Rockwell Science Center – Dr. John Hong
Lockheed Martin – Dr. Char Mo Chen

4.3. Time Wavelength Signal Processing

Scientific Personnel
Prof. Bahram Jalali, Co-P.I.
Dr. Fred Coppinger, postdoc
Dr. Parag Kelkar, posdoc
Bhushan Asuri, Research Assistant
Siva Yegnanarayanan, Research Assistant

Digital Signal Processing (DSP) has revolutionized modern communication and radar systems. For wideband systems, however, the application of DSP is hindered by the difficulty in performing the Analog-to-Digital Conversion (ADC) of wideband signals. A state-of-the-art electronic ADC, embodied by the real-time Tektronix digitizing oscilloscope (Tektronix TDS7404) boasts 20 Gsample/s, 4 GHz analog bandwidth and an Effective Number of Bits (ENOB) of approximately 4.5 bits, over the full bandwidth. The high sampling rate is achieved by using the *time-interleaved* architecture. Here the signal is captured by a parallel array of slow digitizer that are sequentially clocked at a sub-Nyquist rate. The Nyquist criterion is satisfied when the signal is reconstructed in the digital domain. It is well known that the mismatches between digitizers in the array limit the dynamic range, so measured by the ENOB.

Under the MURI program and the subsequent DARPA PACT program, we developed an entirely new A/D architecture. The so-called *time-stretch* ADC, shown in Figure 4.3-1. Here the analog signal is slowed down prior to sampling and digitization by an electronic digitizer. For a time-limited input, a single channel, shown in Figure 1a, suffices. A continuous-time input can be captured with a multi-channel system shown in Figure 1b, where the partitioning of the continuous signal into parallel segments can be performed in the wavelength domain through time-to-wavelength mapping. Slowing down the signal prior to digitization has several advantages. For a stretch factor of M, the effective sampling rate is increased to $M.fs$. The input bandwidth of the electronic digitizer is also increased by M. The error associated with the jitter in the sampling clock of the digitizer is reduced due to a reduction in the signal slew rate. For a time-limited input, only a single digitizer is needed (Figure 4.3-1(a)) hence eliminating the inter-channel mismatch problem. For the continuous-time system (Figure 4.3-1(b)) it has recently been shown that mismatch errors can be corrected using the information available in the signal. This is an important advantage of the *time-stretch* ADC over the *time-interleaved* ADC. It exploits a fundamental difference between the two systems: in the former, the signal at each channel is sampled at or above the Nyquist rate whereas in the latter, it is sampled at a fraction of the Nyquist rate.

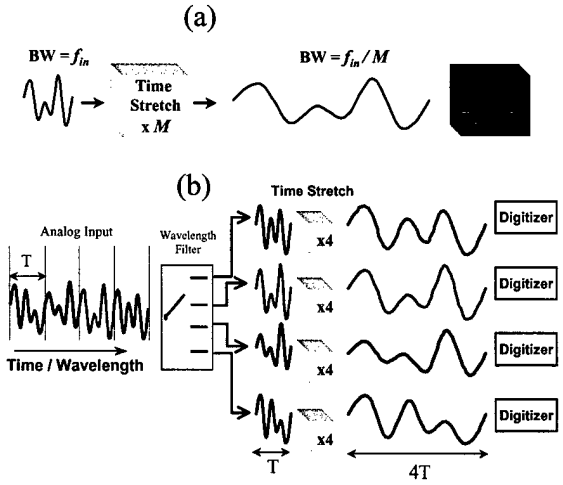

Figure 4.3-1 Time-stretch Analog-to-Digital Conversion. (a) with a time-limited input signal, and (b) with a continuous-time input signal.

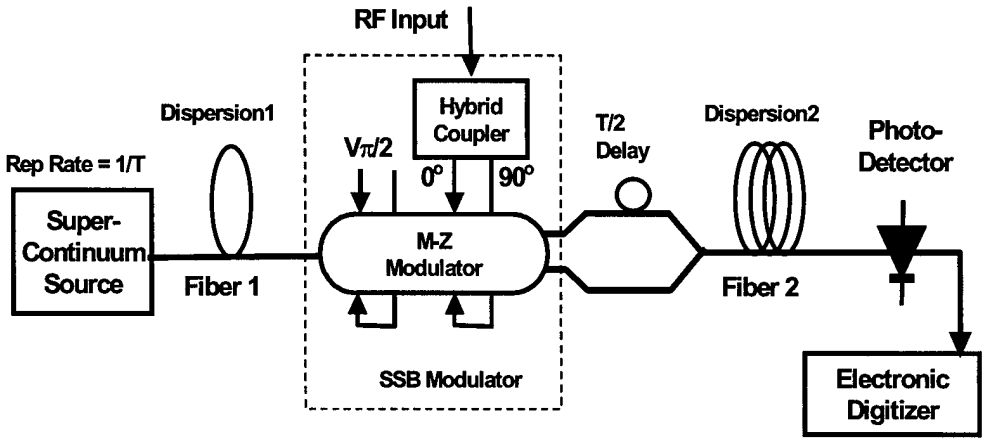

Figure 4.3-2 Physical implementation of the time-stretch preprocessing. Single SideBand (SSB) modulation removes the electrical bandwidth limitation imposed by dispersion. The differential Mach-Zehnder (MZ) modulation is used to remove common-mode distortion.

Figure 4.3-2 shows the physical implementation for a single channel *time-stretch* ADC. The input electrical signal is modulated onto a chirped optical carrier. This is followed by dispersion, leading to temporal stretching of the modulation envelope. A single sideband modulation format eliminates the dispersion penalty that would otherwise place a limit on the electrical bandwidth. While a phase distortion remains, the effect is static and can be filtered in the digital domain. The differential scheme, using dual-output Mach-Zehnder modulator, is used to remove temporal distortions caused by the non-uniform power spectral density of the supercontinuum source and the RIN noise. It is important to note that this system is different than the time-lens, both in theory and in physical implementation. In the time-lens, the input signal must be dispersed. For ADC

applications, the input signal is electrical. The lack of any wideband and low-loss electrical dispersive technology makes it difficult to use the time-lens in ADC applications.

Figure 4.3-3 shows 120 Gsample/s real-time digitization of a 20GHz signal. This was achieved by cascading a 6x photonic time-stretch preprocessor with the 20Gsample/s Tektronix TDS7404 digitizer which has a 4GHz bandwidth. The time-stretch increases the bandwidth to 24GHz making it possible to capture a 20GHz signal with the 4GHz digitizer. Presently, the Signal-to-Noise Ratio (SNR) is 3.5bits over the full 24GHz effective bandwidth. This is one-bit lower than the 4.5 bit resolution of the electronic digitizer. The detailed discussion of this phenomenon is beyond the length-limit of this paper, but simply stated, it originates from partial loading of the digitizer in our experiment. With a modified O-E stage, we expect to recover this reduction in the SNR to the point that it will be limited purely by the electronic digitizer.

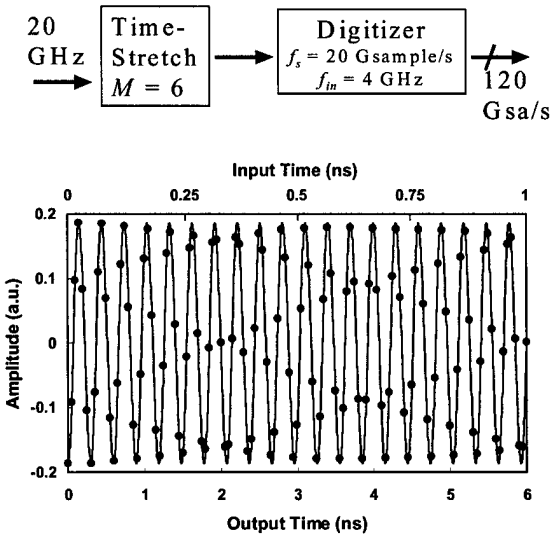

Figure 4.3-3 Experimental demonstration of the time-stretch ADC. Real-time capture of a 20GHz input at 120 Gsample/s is demonstrated. The system has an effective bandwidth of 24 GHz.

Time-frequency techniques can also be used to generate ultra wideband electrical waveforms with arbitrary modulation. In this approach the spectrum of a broadband optical pulse is shaped according to the waveform of interest. Following dispersion, this spectral waveform is directly transformed into an identical time waveform, which is subsequently converted to electronic domain using a photodetector. In a recent demonstration, intelligent digital control of the spectrum has been used to render the system insensitive to the nonuniform power spectral density of the optical source. The system directly converts digital data to ultra wideband analog waveforms.

Technology Transfer

Dr. Fred Coppinger became employed at Harmonic Inc. one of the leading suppliers of analog fiber optic systems to the CATV industry. His knowledge of analog photonics acquired under this program has been instrumental in design of optical video distribution systems. Dr. Parag Kelkar became employed at Corning. Siva Yegnanarayanan and Bhushan Asuri became employed at the Optical Networking Group of Intel Corporation. Aerospace Corp. is planning to construct a time stretch ADC system modeled after UCLA's testbed. UCLA is currently assisting Lawrence Livermore laboratory on development of a time stretch system for capture of ultra fast transients.

4.4. VCSEL's with Intracavity Absorbers

Scientific Personnel
Professor Connie Chang-Hasnain, Co-P.I.
Professor Kam Y. Lau, Co-P.I.

We have demonstrated a variety of applications using a vertical cavity laser with an intracavity absorber/modulator. Independent control of the gain region and the quantum-well absorber allows the device to be used as an integrated optical source and modulator. Experimental demonstration of optical carrier modulation by applying the signal to the intracavity absorber is demonstrated. We achieve a 9 GHz small signal modulation bandwidth and a modulation efficiency of 7GHz/√mA using this technique. Furthermore, our absorber modulation technique is expected to result in less frequency chirping than does direct gain modulation. Our novel device is a vertical cavity surface emitting laser with an n-p-n configuration that has an additional quantum well integrated into the upper mirror stack, as shown in Figure 4.4-1.

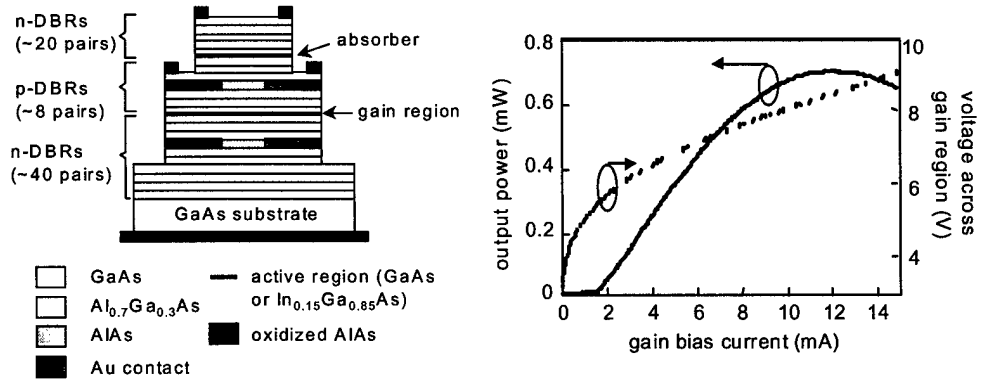

Figure 4.4-1 Schematic structure of VCSEL with an intracavity absorber and its light-versus-current characteristics with 0V applied on the absorber.

The response of the device to absorber modulation is shown in Figure 4.4-2, for a variety of gain bias conditions. We achieve a small signal modulation bandwidth of 9 GHz at a gain bias current of 8 mA and a modulation depth of 0.6%. As expected, the small-signal

modulation bandwidth increases as the square root of the gain current bias above threshold. The bandwidth efficiency of the absorber modulation technique (7 GHz/√mA) is comparable to that obtained using direct gain modulation. Furthermore, the absorber modulation bandwidth is relatively independent of the choice of DC absorber bias.

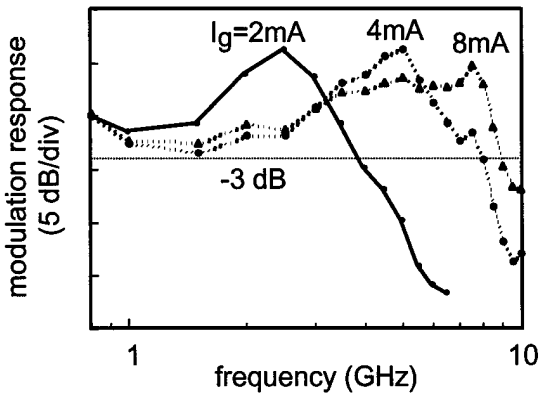

Figure 4.4-2 Absorber modulation response for varying DC gain bias currents (I_g). The DC absorber bias $V_{a,DC}$ = 1 V, and the small-signal AC modulation of the absorber voltage is -10 dBm.

5. Planar Antennas for Photonic-Microwave Conversion

Scientific Personnel
Professor Tatsuo Itoh, Co-P.I.
Yongxi Qian, Postdoctoral Researcher
Noriaki Kaneda, Research Assistant

High-power, high-frequency photodetectors can significantly reduce RF insertion loss, increase spurious-free dynamic range, and enhance system signal-to-noise ratio. They are also imperative for the generation of millimeter-wave and THz frequency power by optical heterodyning. In addition to the development of novel photonic devices, we believe that the overall performance of microwave-photonics systems can greatly benefit by the integration of such devices with antennas. If the microwave power is delivered to an antenna load free-space power combining can be used. Research done in the investigator's group has been focused on the integration of active microwave devices with planar antennas. In this scenario antennas are utilized as power combiners/splitters, harmonic tuners, and mode filters, as well as acting as the radiating element. This offers a tremendous savings in overall circuit size and insertion loss, which becomes a serious concern at millimeter-wave frequencies. The same benefits can be obtained by the integration of antennas and microwave-photonic devices such as velocity-matched distributed photodetector (VMDP).

Our research effort has been to develop antennas which are compatible with microwave-photonic devices. There are three main challenges that are addressed: 1. Fabrication on semi-conductor materials (GaAs, InP), 2. Antenna efficiency, 3. Excitation mechanism

of antenna. Antennas printed on high dielectric constant substrates such as GaAs and InP typically suffer from undesired affects due to generation of surface-waves, including low radiation efficiency, high cross-pol radiation, and strong mutual coupling.

The novel printed quasi-Yagi antenna was developed to take advantage of the generation of surface-waves, making it ideal for construction on III-V materials. The printed antenna configuration is very similar to the configuration of the Yagi-Uda dipole array in such a way that all three dipole components, which include the driver dipole, director dipole and the reflector, can be readily identified. However, the role of the driver dipole has become the generator of surface-wave power in the high dielectric substrate on which the antenna is printed. The generated TE0 surface-wave energy directly contributes to free-space radiation. The endfire nature of the antenna comes in part due to the truncated microstrip ground plane on the backside of the substrate that acts as an ideal reflector for the TE0 mode. Because they share the same field polarization the TE0 surface-wave is strongly coupled to the parasitic director dipole element of the quasi-Yagi antenna, influencing the antenna's radiation pattern and impedance bandwidth. A photograph of an X-band (8-12 GHz) prototype of the antenna fabricated on 0.635 mm RT/Duroid with permittivity of 10.2 is shown in Figure 4.4-1.

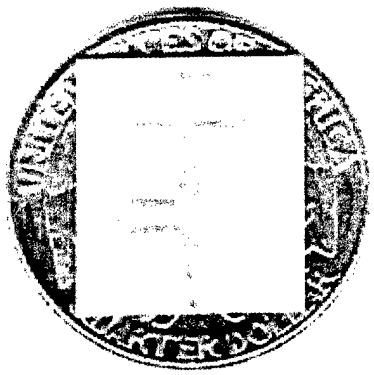

Figure 4.4-1 Photograph of fabricated X-band quasi-Yagi antenna.

Measured results show that the quasi-Yagi antenna radiates an endfire beam, with a front-to-back ratio better than 15 dB with cross-pol less than -12 dB across a large frequency range (50%). Antenna radiation efficiency was measured to be 93%. This planar antenna will also be beneficial in the design of phased array antennas due to its broad main beam, compact size, and low mutual coupling (<-22 dB). Additionally, the antenna is easily scaled to cover various frequency bands. This has been experimentally verified at C-band (4-6 GHz) and V-band (50 -75 GHz) with no difficulties. In addition, measurement of the radiation efficiency of the antenna structure shows peak efficiency greater than 90%.

For integrating of the quasi-Yagi antenna and the VMDP instead of the single microstrip feeding, coupled microstrip feeding is employed to provide complete compatibility and integration of the two components (Figure 4.4-2).

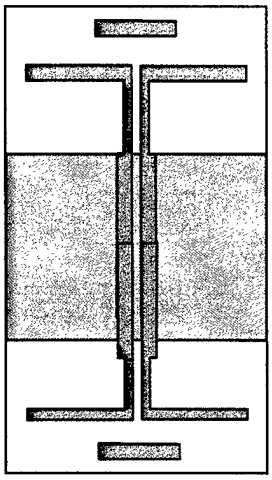

Figure 4.4-2 Schematic of quasi-Yagi back-to-back coupled microstrip line to waveguide transition.

We rely on the odd-symmetric nature of the VMDP to generate the balanced field configuration needed to excite the driver dipole. In addition, this structure is able to provide heat sinking through the metal backing under the coupled lines while still ensuring broad band operation and unidirectional radiation. The X-band prototype of the back-to-back coupled line-to-waveguide transition exhibits a bandwidth of 26% for return loss less than –10dB. The insertion loss ranges from –0.5 to –1.2 dB. This structure can be readily scaled to other frequency ranges and be optimized for an increase in operational bandwidth (Figure 4.4-3).

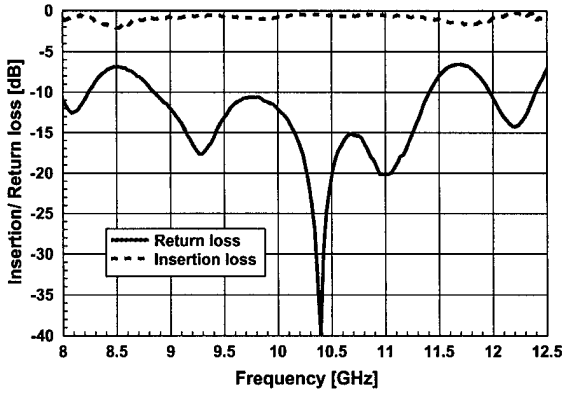

Figure 4.4-3 Measured results of back-to-back coupled microstrip line to waveguide transition.

The same antenna structure has been successfully demonstrated as a low loss microstrip-to-waveguide transition which exhibits a 35% bandwidth with return loss better than -12 dB and insertion loss -0.3 dB at X-band frequencies. Measurements of a V-band (50-75 GHz) transition show a 30% bandwidth with return loss better than -10 dB with 95% transmission efficiency at the center of the band (Figure 4.4-4).

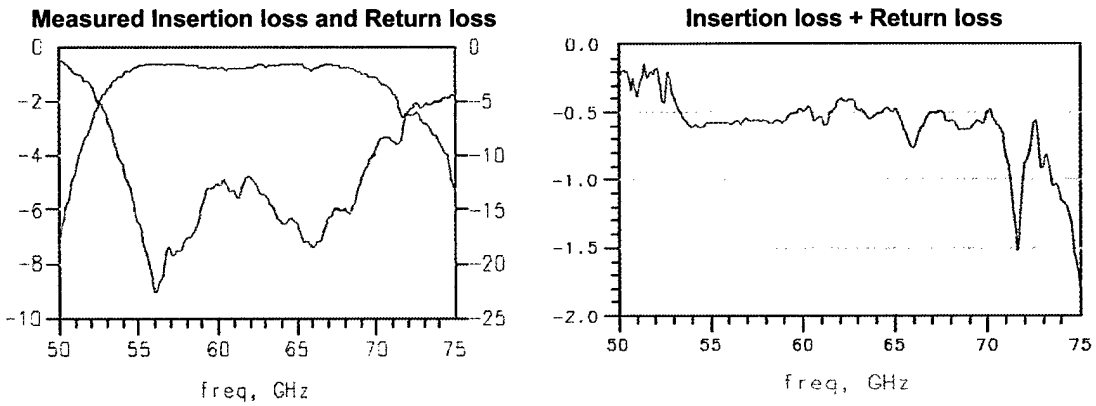

Figure 4.4-4 Measured insertion loss, return loss, and efficiency of back-to-back waveguide to microstrip transition using quasi-Yagi antenna.

The development of the integrated antennas and waveguide transitions can be used for power combining at microwave frequencies. Power can be collected in metallic waveguides or be launched directly into free-space for applications such as in quasi-optical power combining.

6. Publications and Presentations

6.1. Photodetectors and Modulators

1. P. K. L. Yu and M. C. Wu, "Photodiodes for High Performance Analog Links," in *RF Photonic Technology in Optical Fiber Links*, W. S. C. Chang, Editor, Cambridge University Press, Cambridge, UK, 2002.

2. * Sanjeev Murthy, Seong-Jin Kim, Thomas Jung, Zhi-Zhi Wang, Wei Hsin, T. Itoh, and Ming C. Wu, "Backward Wave Cancellation in Distributed Traveling Wave Photodetectors," IEEE Journal of Lightwave Technology, Vol. 21, No. 12 , pp. 3071-3077, Dec. 2003 (Invited Paper)

3. Murthy, S.; Jung, T.; Wu, M.C.; Sivco, D.L.; Cho, A.Y., "Traveling wave distributed photodetectors with backward wave cancellation for improved AC efficiency," Electronics Letters, Vol. 38, No. 15, pp. 827 –829, July 2002.

4. M.S. Islam, T. Jung, T. Itoh, M.C. Wu, A. Nespola, D.L. Sivco, and A.Y. Cho, "High power and highly linear monolithically integrated distributed balanced photodetectors," Journal of Lightwave Technology, vol.20, (no.2), p.285-295, February 2002.

5. S. Mathai, F. Cappelluti, T. Jung, D. Novak, R.B. Waterhouse, D. Sivco, A.Y. Cho, G. Ghione, M.C. Wu, "Experimental demonstration of a balanced electroabsorption modulated microwave photonic link," IEEE Transactions on Microwave Theory and Techniques, Vol. 49, No. 10, pp. 1956 -1961, Oct 2001.

6. S. Mathai, F. Cappelluti, T. Jung, D. Novak, R. Waterhouse, D.L. Sivco, A.Y. Cho, G. Ghione, M.C. Wu, "Simultaneous Suppression of Laser Relative Intensity Noise, 2^{nd} and 3^{rd} order distortions Using a Balanced Electroabsorption Modulator," SPIE Annual Meeting: International Symposium on Optical Science and Technology, 29 July 3 Aug. 2001.

7. S. Mathai, T. Jung, F. Cappelluti, D. Novak, R. Waterhouse, G. Ghione, D. Sivco, A.Y. Cho, M.C. Wu, "Experimental demonstration of a balanced electroabsorption modulator," International Topical Meeting on Microwave Photonics Technical Digest (MWP 2000) Postdeadline Papers, Oxford, UK, 11-13 Sept. 2000. Received Best Student Paper Award.

8. F. Cappelluti, S. Mathai, M.C. Wu, G. Ghione, "Balanced Electroabsorption Modulator for High-Linearity, Low-Noise Microwave Analog Optical Link," Proceedings of the Gallium Arsenide and Other Semiconductor Applications Symposium (GAAS 2000), Paris, France, 1-6 Oct. 2000.

9. F. Cappelluti, S. Mathai, M.C. Wu, G. Ghione, "Balanced Electroabsorption Modulated RF Photonic Link," Conference on Lasers and Electro-Optics Europe Technical Digest (CLEO/Europe 2000), Nice, France, 10-15 Sept. 2000.

10. F. Cappelluti, S. Mathai, M.C. Wu, G. Ghione, "Microwave Analog Optical Link Using a Balanced Electroabsorption Modulator," Proceedings of the 3rd International Summer School on Interactions Between Microwave and Optics (OMW 2000), Autrans, France, 28 August - 1 Sept. 2000.

11. F. Cappelluti, S. Mathai, G. Ghione, M.C. Wu, "High performance RF phtonic link using a balanced electroabsorption modulator," Proceedings of the Tenth Annual DARPA

12. M.S. Islam, S. Murthy, T. Itoh, M.C. Wu, D. Novak, R. Waterhouse, D.L. Sivco, and A.Y. Cho, "Velocity-matched Distributed Photodetectors and Balanced Photodetectors with p-i-n Photodiodes," accepted for publication in *IEEE Transactions on Microwave Theory and Techniques,* Special issue on RF Photonics, Oct. 2001.

13. M.S. Islam, T. Jung, A. Nespola, T. Itoh, M.C. Wu, D.L. Sivco, and A.Y. Cho, "High Power and Highly Linear Monolithically Integrated Distributed Balanced Photodetectors," accepted for publication in *IEEE/OSA Journal of Lightwave Technology*, 2001.

14. M.S. Islam, T. Chau, T. Itoh, M.C. Wu, D.L. Sivco, and A.Y. Cho, "Distributed Balanced Photodetectors," Selected Topics in High Speed Electronics and Systems, World Scientific, 1999 (Book Chapter)

15. M.S. Islam, Tai Chau, Tatsau Itoh, M.C. Wu, D.L. Sivco, and A.Y. Cho, "Distributed balanced photodetectors for improved performance in RF photonic systems," *Int. Jour. of High-Speed El. and Sys.,* World Scientific, 1999. (Invited paper)

16. M.S. Islam, T. Chau, S. Mathai, T. Itoh, M.C. Wu, D.L. Sivco, and A.Y. Cho, "Distributed Balanced Photodetectors for Broadband Noise Suppression," IEEE Transactions on Microwave Theory and Techniques, 47, (7), pp 1282-88, July, 1999.

17. M.S. Islam, T. Chau, S. Mathai, A. Rollinger, A. Nespola, T. Itoh, M.C. Wu D.L. Sivco, and A.Y. Cho, "Distributed balanced photodetectors for high performance RF photonic links," IEEE Photonics Technology Letters, 11, (4), pp 454-7, April, 1999.

18. M.S. Islam, "Distributed balanced photodetectors" LEOS Annual Meeting, 2001 (invited paper).

19. M.S. Islam, A. Nespola, M. Yeahia, M.C. Wu, D.L. Sivco, and A.Y. Cho, "Correlation Between the Failure Mechanism and Dark Currents of High Power Photodetectors," Submitted to LEOS Annual Meeting, 2000.

20. M.S. Islam, M.C. Wu, D.L. Sivco, and A.Y. Cho, "Distributed Balanced Photodetectors with p-i-n Photodiodes for Broadband Suppression of Laser Noise," OSA annual meeting, Rhode Island, USA, 2000.

21. M.S. Islam, T. Jung, S. Murthy, T. Itoh , M.C. Wu, D.L. Sivco, and A.Y. Cho "Velocity-matched distributed photodetectors with p-i-n photodiodes," Int.Top. Meeting on Microwave Photonics 2000, Oxford, UK, Sept. 11-13, 2000.

22. M.C. Wu, M.S. Islam, S. Murthy, T. Jung, and T. Chau, "High Power Millimeter-Wave Photodetectors," Int. Topical Meeting on Microwave Photonics, 2000, Oxford, UK, Sept. 11-13, 2000. (Invited paper)

23. M.S. Islam, T. Jung, S. Mathai, T. Chau, T. Itoh, M.C. Wu, D.L. Sivco, and A.Y. Cho, "High Power Distributed Balanced Photodetectors with High Linearity," Int. Topical Meeting on Microwave Photonics, Melbourne, Australia, Nov.16-19, 1999.

24. M.S. Islam, T. Chau, S. Mathai, T. Itoh, M.C. Wu, D.L. Sivco, and A.Y. Cho " Experimental Investigation of Power Distribution in Distributed Balanced Photodetectors," LEOS '99 annual meeting, San Francisco, CA, Nov. 8-11, 1999.

25. M.C. Wu, T. Chau, M.S. Islam, "High speed velocity matched distributed photodetector," LEOS '99 annual meeting, San Francisco, CA, Nov 8-11, 1999. (Invited talk)

26. M.S. Islam, T. Chau, T. Itoh, M.C. Wu, D.L. Sivco, and A.Y. Cho, "Distributed Balanced Photodetectors for RF Photonic links," SPIE Conference Proc. on Terahertz and Gigahertz Photonics, Denver, CO, July 19-23, 1999. (Invited paper)

27. M.C. Wu, M.S. Islam, and T. Chau, "Distributed Balanced Photodetectors for High Performance RF Photonoc Applications," 1999 Advanced Workshop on Frontiers in Electronics (WOFE) 1999 Lecce, Italy: May 31 - June 4, 1999. (Invited paper)

28. M.S. Islam, T. Chau, S. Mathai, T. Itoh and M.C. Wu, "Noise Suppression Properties of Distributed Balanced Photodetectors for High Performance RF Photonic Links," Conference on Laser and Electro-optics (CLEO), Baltimore, MD, May 23-28, 1999.

29. M.S. Islam, T. Chau, S. Mathai, A. Rollinger, X.J. Meng, T. Itoh and M.C. Wu, "Monolithic Integration of Distributed Balanced Photodetectors for High Performance RF Photonoc Links," OFC '99, San Diego, CA, Feb. 1999.

30. M.S Islam, Tai Chau, S. Mathi, A. R. Rollinger, W.R. Deal, T. Itoh and M.C. Wu, "Monolithic Integration of Distributed High Power Balanced Photodetectord for Shot-Noise Limited Performance," Multi University Research Initiative (MURI) Annual Review Meeting, Los Angeles, CA, Oct 22, 1998.

31. M.C. Wu, T. Itoh, T. Chau, M.S. Islam, S. Mathai, A. Rollinger, "High Power Photodetectors," International Topical Meeting on Microwave Photonics, Sarnoff Corporation, Princeton, New Jersey, Oct. 12-14, 1998.

32. M.S. Islam, T. Chau, S. Mathai, A. Rollinger, A. Nespola, W.R. Deal, T. Itoh and M.C. Wu, "Distributed Balanced Photodetectors for RF Photonoc Links," Int.Topical Meeting on Microwave Photonics, Princeton, NJ, 12-14 Oct.1998.

33. Tai Chau, M.S. Islam, S. Mathai, A. Rollinger, A. Nespola, L. Fan. T. K. Tong, W.R. Deal, T. Itoh and M.C. Wu, D. C. Scott, T.A. Vang, L. Lembo, J. Elliott, D.L. Sivco and A.Y. Cho "Long Wavelength Velocity-Matched Distributed Photodetectors," The 1998 Annual Research Symposium, UCLA, Covell Commons, Los Angeles, CA, Feb. 24-25, 1998.

34. M.S. Islam, T. Chau, A. Nespola, S. Mathi, A.R. Rollinger, D.T.K. Tong, W.R. Deal, T. Itoh and M.C. Wu, "Distributed High Power Balanced Photodetectors for Shot-Noise Limited Performance," Multi University Research Initiative Annual Review Meeting, UCLA, Los Angeles, CA, December 11-12, 1997.

6.2. Electro-Optic Polymer Modulators

1. "Three dimensional integrated optics using polymers", S. M. Garner,S-S Lee, V. Chuyanov, A. Chen, A. Yacoubian, W. H. Steier, IEEE J. Quant. Electr. vol. 35, pp 1146-1155, 1999

2. "Recent advances in polymer electro-optic devices for photonics" (Invited), W. H. Steier, S-S Lee, S. Garner, A. Chen, H. Zhang, V. Chuyanov, H. R. Fetterman, A. Udupa, D. Bhattacharya, D. Chen, L. R. Dalton, Chemical Physics, vol. 245, pp 487-506, 1999

3. "Vertically integrated waveguide polarization splitters using polymers" S. Garner, V. Chuyanov, S-S Lee, A. Chen, W. H. Steier, L. R. Dalton, IEEE Phot. Tech. Lett.,11, 842-4,(1999).

4. "Integrated optical polarization splitter based on photo-bleaching induced birefringence in azo dye polymers", S-S Lee, S. Garner, W. H. Steier, S-Y Shin, accepted for publication in Applied Optics.

5. "High frequency polymer modulators with integrated finline transitions and low V ", D. Chen, D. Bhattacharya, A. Udupa, B. Tsap, H. R. Fetterman, A. Chen, S-S Lee, J. Chen, W. H. Steier, L. R. Dalton, IEEE Phot. Tech. Lett., 11, 54-56, (1999)

6. "The Molecular and Supramolecular Engineering of Polymeric Electro-Optic Materials,"(invited) ,B. H. Robinson, L. R. Dalton, A. W. Harper, A. Ren, F. Wang, C. Zhang, G. Todrova, M. Lee, R. Aniszfeld, S. M. Garner, A. Chen, W. H. Steier, S, Houbrecht, A. Persoons, I. Ledoux, J. Zyss, and A. K. Y. Jen, Chem. Phys., vol. 245, pp 35-50, 1999

7. "Thermoset Second-Order NLO Materials from a Trifunctionalized Chromophore," Y. S. Ra, S. S. H. Mao, B. Wu, L. Guo, A. Chen, and W. H. Steier, Organic Thin Films, ACS Symposium Series 695 (C. W. Frank, ed.) Amer. Chem. Soc., Washington, DC, 1998, 288-94.

8. "Design and Synthesis of a Perfluoroalkyldicyano-vinyl-Based NLO Material for Electro-Optic Applications," F. Wang, A. W. Harper, M. He, A. Ren, L. R. Dalton, S. M. Garner, A. Yacoubian, A. Chen, and W. H. Steier, Organic Thin Films, ACS Symposium Series 695 (C. W. Frank, ed.) Amer. Chem. Soc., Washington, DC, 1998, 252-7.

9. "Progress Towards the Transition of Large Microscopic Nonlinearities to Large Macroscopic Nonlinearities for High- Materials," M. He, J. Zhu, A. W. Harper, S. S. Sun, L. R. Dalton, S. M. Garner, A. Chen, and W. H. Steier, Organic Thin Films, ACS Symposium Series 695 (C. W. Frank, ed.) Amer. Chem. Soc., Washington, DC, 1998, 258-66.

10. "Demonstration of a photonically controlled rf phase shifter", S-S Lee, A. H. Udupa, H. Erlig, H. Zhang, Y. Chang, C. Zhang, D. H. Chang, D. Bhattacharya, B. Tsap, W. H. Steier, L. R. Dalton, H. R. Fetterman, IEEE Microwave and Guided Wave Lett., 9, pp357-9, (1999)

11. "Investigation on new polyurethane and incorporation of a soluble high chromophore for electro-optic applications", C. Zhang, C. Wang, L. R. Dalton, G. Sun, H. Zhang, W. H. Steier, Am. Chem. Soc. Anahiem, CA 1999

12. "Thermally Stable Polyene-Based NLO Chromophore and Its Polymers with Very High Electro-Optical Coefficients",Cheng Zhang, Albert S. Ren, Fang Wang, Larry R. Dalton, Sang-Shin Lee, Sean M. Garner, William H. Steier Polym. Prepr. vol. 40, 49 (1999)

13. "High-frequency, low crosstalk modulator arrays based on FTC polymer systems", A. H. Udupa, H. Erlig, B. Tsap, Y. Chang, D. Chang, H. R Fetterman, H. Zhang, S-S Lee, F. Wang, W. H. Steier, L. R. Dalton, Electronic Lett., 35, p1702-1704 (1999)

14. "Progress toward device-quality second-order nonlinear optical materials: 4. A tri-link high NLO chromophore in thermoset polyurethane – A "guest-host" approach to larger electro-optic coefficients" C. Zheng, C. Wang, L. R. Dalton, H. Zhang, W. H. Steier, Macromolecules 34, 253-61 (2001)

15. "Production of High Bandwidth Polymeric Electro-Optic Modulators With V Voltages of Less Than 1 Volt". L. R. Dalton, B. Robinson, W. Steier accepted in Molecular Crystals Liquid Crystals Science & Technology Section B. Nonlinear Optics (Materials Research Society) pp1-12. (2000)

16. L. R. Dalton, B. Robinson, W. H. Steier, C. H. Zhang, and G. Todorova, "Systematic Optimization of Polymeric Electro-Optic Materials," Proc. SPIE, 4114, 65-76 (2001)

17. Hua Zhang, M-C Oh, A. Szep W. H. Steier, C. Zhang, L. R. Dalton, H. Erlig, Y. Chang, D. H. Chang, H. R. Fetterman, "Push Pull Electro-optic Polymer Modulators with Low Half-Wave Voltage and Low Loss at both 1310 nm and 1550 nm" Appl. Phys. Lett. 78, p3116 –8 (2001)

18. M-C. Oh, H. Zhang, A. Szep , W. H. Steier, C. Zhang, L. R. Dalton, H. Erlig, Y. Chang. Boris Szep, H. R. Fetterman, "Recent advances in electro-optic polymer modulators incorporating phenyltetraene bridged chromophore " (Invited) J. Quant Electr. Sel. Topics on Organics for Photonics, 7, pp826-35,(2001)

6.3. Time Wavelength Signal Processing

1. F. Coppinger, A.S. Bhushan, and B. Jalali, "Time magnification of electrical signals using chirped optical pulses," Electronics Letters, Vol. 34 (no.4), pp. 399-400, February 1998.

2. A.S. Bhushan, F. Coppinger, B. Jalali, S. Wang, and H.F. Fetterman, "150 Gsample/s wavelength division sampler with time-stretched output," Electronics Letters, Vol. 34 (no.5), pp. 474-5, March 1998.

3. A.S. Bhushan, F. Coppinger, and B. Jalali, "Time-stretched analogue-to-digital conversion," Electronics Letters, Vol. 34 (no.11), pp. 1081-3, May 1998.

4. B. Jalali, F. Coppinger, and A.S. Bhushan, "Photonic time-stretch offers solution to ultrafast analog-to-digital conversion," Optics in 1998, Optics and Photonics News, pp. 31-2, December 1998.

5. B. Jalali, F. Coppinger, and A.S. Bhushan, "Time-stretch preprocessing overcomes ADC limitations," Microwaves & RF Magazine, Vol. 38 (no.3), pp. 57-66, March 1999.

6. F. Coppinger, C.K. Madsen, and B. Jalali, "Photonic microwave filtering using coherently coupled integrated ring resonators," Microwave and Optical Technology Letters, Vol. 21 (no.2), pp. 90-3, April 1999.

7. B. Jalali, F. Coppinger, and A.S. Bhushan, "Photonic preprocessing for analog-to-digital conversion of ultrafast signals", Optical Processing & Computing, SPIE's International Technical Group Newsletter, Photonics and Phased Array Systems," Vol. 10 (no.1), pp. 1-2, April 1999.

8. B. Jalali, F. Coppinger, and A.S. Bhushan, "Time-stretch methods capture fast waveforms," Microwaves & RF Magazine, Vol. 38 (no.4), pp. 63-9, April 1999.

9. A.S. Bhushan, F. Coppinger, S. Yegnanarayanan, and B. Jalali, "Nondispersive wavelength-division sampling," Optics Letters, Vol. 24 (no.11), pp. 738-40, June 1999.

10. F. Coppinger, A.S. Bhushan, and B. Jalali, "Photonic time stretch and its application to analog-to-digital conversion," Transactions on Microwave Theory and Techniques, Vol. 47 (no.7), pp. 1309-14, July 1999.

11. F. Coppinger, A.S. Bhushan, and B. Jalali, "Time reversal of broadband microwave signals", Electronics Letters, Vol. 35 (no.15), pp. 1230-2, July 1999.

12. P.V. Kelkar, F. Coppinger, A.S. Bhushan, and B. Jalali, "Time-domain optical sensing," Electronics Letters, Vol. 35 (no.19), pp. 1661-2, September 1999.

MURI / DARPA PACT Patents

13. "Data Conversion Using Time Manipulation" US #6,288,659 - Granted 09/11/01 – USA, Bahram Jalali, Fred Coppinger (UC Regents).

14. "Method and Apparatus for Arbitrary Waveform Generation Using Photonics" US # 6,724,783 – Granted 04/20/04 – USA, Bahram Jalali, Parag Kelkar (UC Regents).

6.4. Planar Antennas for Photonic-Microwave Conversion

1. B.-S. Ke, T. Chau, Y. Qian, M. C. Wu, and T. Itoh, "Tapered slot antenna integrated with velocity matched distributed photodetector," International Microwave Symposium Digest, vol. 3, pp. 1241-1244, June 1998.

2. N. Kaneda, Y. Qian, and T. Itoh, "A Broadband Microstrip-to-Waveguide Transition using quasi-Yagi Antenna, "IEEE Transactions on Microwave Theory Tech., vol. 47, No. 12, pp. 2562-2567, December 1999.

3. W. R. Deal, N. Kaneda, J. Sor, Y. Qian, and T. Itoh, "A New Quasi-Yagi Antenna for Planar Active Antenna Arrays, "IEEE Transactions on Microwave Theory Tech., vol. 48, No. 6, pp. 910-918, June 2000.

4. K. M. K. H. Leong, S. S. Murthy, N. Kaneda, Y. Qian, M. C. Wu, and T. Itoh, "Planar Antennas for Microwave Photonics," Topical Meeting on Microwave Photonics, pp. 219-222, Jan. 2002.

5. N. Kaneda, Y. Qian and T. Itoh, "A broadband microstrip-to-waveguide transition using quasi-Yagi antenna", IEEE Transactions on Microwave Theory and Techniques, vol. 47, no. 9, pp. 2562-2567, Dec. 1999.

6. Y. Qian, W.R. Deal, N. Kaneda and T. Itoh, " A microstrip-fed quasi-Yagi antenna with broadband characteristics", Electronics Letters, vol. 34, no. 23, pp. 2194-2196, Nov. 1998.

7. N. Kaneda, Y. Qian and T. Itoh, "A broadband CPW-to-waveguide transition using quasi-Yagi antenna", to be presented in 2000 IEEE MTT-S International Microwave Symposium, Boston, MA, June. 2000.

8. T. Chau, N. Kaneda, T. Jung, A. Rollinger, S. Mathai, Y. Qian, T. Itoh, M. C. Wu, B. Shillue, J. Payne and D. Emerson, "High speed Velocity-Matched Distributed Photodetectors", 1999 IEEE LEOS Annual Meeting Conference Proceedings, San Francisco, CA, pp. 834-835, Nov. 1999.

9. Y. Qian, W.R. Deal, N. Kaneda and T. Itoh, " A uniplanar quasi-Yagi antenna with wide bandwidth and low mutual coupling characteristics", 1999 IEEE AP-S International Symposium Digest, Orlando, FL, Vol. 2, pp. 924-927, July. 1999.

10. N. Kaneda, Y. Qian and T. Itoh, "A broadband microstrip-to-waveguide transition using quasi-Yagi antenna", 1999 IEEE MTT-S International Microwave Symposium Digest, Anaheim, CA, Vol. 4, pp. 1431-1434, June. 1999.

11. N. Kaneda, Y. Qian and T. Itoh, "A novel Yagi-Uda dipole array fed by a microstrip-to-CPS transition", 1998 Asia-Pacific Microwave Conference Proceedings, Yokohama, Japan, pp. 1413-1416, Dec. 1998.

6.5. Novel Photonic Systems

1. Lam, C.F.; Vrijen, R.B.; Chang-Chien, P.P.L.; Sievenpiper, D.F.; Yablonovitch, E. "A tunable wavelength demultiplexer using logarithmic filter chains," Journal of Lightwave Technology, vol.16, (no.9), IEEE, Sept. 1998. p.1657-62.

2. Sievenpiper, D.F.; Lam, C.F.; Yablonovitch, E. "Two-dimensional photonic-crystal vertical-cavity array for nonlinear optical image processing," Applied Optics, vol.37, (no.11), Opt. Soc. America, 10 April 1998. p.2074-8.

3. Rendina, I.; Coppinger, F.; Jalali, B.; Lam, C.; Yablonovitch, E. "Coupled-cavity distributed-resonance photodetectors," Proceedings of the SPIE - The International Society for Optical Engineering, vol.3278, (Integrated Optic Devices II, San Jose, CA, USA, 28-30 Jan. 1998.) SPIE-Int. Soc. Opt. Eng, 1998. p.293-304.

4. Lam, C.F.; Yablonovitch, E. "A fast wavelength hopped CDMA system for secure optical communications," Proceedings of the SPIE The International Society for Optical Engineering, vol.3228, (Multimedia Networks: Security, Displays, Terminals, and Gateways, Dallas, TX, USA, 4-5 Nov. 1997.) SPIE-Int. Soc. Opt. Eng, 1998. p.390-8.

5. Lam, C.F.; Vrijen, R.; Tong, D.T.K.; Wu, M.C.; Yablonovitch, E. "Spectrally encoded CDMA system using Mach-Zehnder encoder chains," Proceedings of the SPIE - The International Society for Optical Engineering, vol.3228, (Multimedia Networks: Security, Displays, Terminals, and Gateways, Dallas, TX, USA, 4-5 Nov. 1997.) SPIE-Int. Soc. Opt. Eng, 1998. p.399-407.

6. Lam, C.F.; Yablonovitch, E. "Terabit switching and security enhancement in a WDM/TDM hybrid system," 1997 Digest of the IEEE/LEOS Summer Topical Meetings, Canada, 11-15 Aug. 1997. p.20-1.

7. Lam, C.F.; Yablonovitch, E. "A configurable wavelength demultiplexer using periodic filter chains," 1997 Digest of the IEEE/LEOS Summer Topical Meetings, Montreal, Que., Canada, 11-15 Aug. 1997.), 1997. p.78-9.

8. Lam, C.F.; Yablonovitch, E. "Multi-wavelength, optical code-division-multiplexing based on passive, linear, unitary, filters," Proceedings 1995 URSI International Symposium on Signals, Systems, and Electronics. ISSSE '95, 1995. p.299-302.

9. Adit Narasimha, X.J. Meng, C.F. Lam, M.C. Wu and E. Yablonovitch, "Maximizing the spectral efficiency of WDM systems by microwave domain filtering of tandem single sidebands," IEEE Transactions on Microwave Theory & Techniques, vol.49, no.10, pt.2, Oct. 2001, pp.2042-7.

10. Adit Narasimha, X.J. Meng, M.C. Wu and E. Yablonovitch, "A tandem single sideband modulation scheme to double the spectral efficiency of analog fiber links," Electronics Letters, vol. 36, no. 13, pp. 1135-1136, 22 June 2000.

11. Adit Narasimha, X.J. Meng, M.C. Wu and E. Yablonovitch, "Full optical spectral utilization by microwave domain filtering of tandem single sidebands," paper WDD44, OFC Technical Digest Series, Conference Edition, Anaheim CA, March 2001.

12. Adit Narasimha, X.J. Meng, M.C. Wu and E. Yablonovitch, "A tandem single sideband fiber optic system using a dual-electrode Mach-Zehnder modulator," paper CMR6, Technical Digest of IEEE/OSA Conference on Lasers & Electro Optics, San Francisco CA, May 2000.

13. Adit Narasimha and E. Yablonovitch, "Code-selective RF photonic mixing for use in optical CDMA demultiplexers," to be presented as paper TuO5 at IEEE LEOS, San Diego CA, November 2001.

14. Alvarado-Rodriguez I, Yablonovitch E. "Separation of radiation and absorption losses in two-dimensional photonic crystal single defect cavities," Journal of Applied Physics, vol.92, no.11, 1 Dec. 2002, pp.6399-402.

15. Wu Pu-Wei, Cheng Wei, Martini IB, Dunn B, Schwartz BJ, Yablonovitch E. "Two-photon photographic production of three-dimensional metallic structures within a dielectric matrix," Advanced Materials, vol.12, no.19, 2 Oct. 2000, pp.1438-41.

16. Boroditsky M, Vrijen R, Krauss TF, Coccioli R, Bhat R, Yablonovitch E. "Spontaneous emission extraction and Purcell enhancement from thin-film 2-D photonic crystals," Journal of Lightwave Technology, vol.17, no.11, Nov. 1999, pp.2096-112.

Recent Graduates with MURI Support:

Professor Ming C. Wu:

Dennis Tong	Ph.D.	1998 (Professor at Hong Kong University of Science and Technology)
Tai Chau	Ph.D.	2000 (at Raytheon)
Andrew Rollinger	Masters	2000 (at Raytheon)
Saif Islam	Ph.D	Spring 2001 (Professor at UC Davis)
Thomas Jung	Masters	current student continuing to PhD
Sagi Mathai	Masters	current student continuing to PhD
Federica Cappelluti	Visiting Student at UCLA for PhD from Politecnico di Torino, Dip. Di Electronica, Torino, Italy	

Professor Tatsuo Itoh:

Noriaki Kaneda	Ph.D.	2000

Professor Eli Yablonovitch:

Dan Sievenpiper	Ph.D.	March 1999 (at HRL)
Cedric Lam	Ph.D.	March 1999
Romolo Broas	Masters	September 1999
Tom Chu	Masters	September 1999
Adit Narasimha	Ph.D.	Fall 2004 (Expected)

Professor Harold Fetterman:

Md. Ershad Ali	Ph.D.	(now at Agilent)
Mihail Milkov	MS	
Dan Chang	Ph.D.	(at JPL)
Ilya Poberezhskiy	MS	Continuing for Ph.D
Talal Azfar	Ph.D.	in progress

Professor William Steir – USC

Antao Chen,	Ph.D.	1998
Vadim Chuyanov,	Ph.D.	1990
Payam Rabiei,	Ph.D.	

Professor Rajeev Ram - MIT:

Steve Patterson	Ph.D.	September 2000
Harry Lee	MS	February 2001

7. Acknowledgment

We like to thank the support of Office of Naval Research under contract # N00014-97-1-0508. We also like to thank the valuable suggestions from Drs. William Miceli, Steve Pappert, William Schneider, and our Scientific Advisory Board; and the hard work of our graduate students.